

**Benzobisthiazole–Thiophene Copolymer
Semiconductors: Synthesis, Enhanced Stability,
Field-Effect Transistors, and Efficient Solar Cells**

Eilaf Ahmed, Felix S. Kim, Hao Xin, and Samson A. Jenekhe*

Department of Chemical Engineering and
Department of Chemistry, University of Washington,
Seattle, Washington 98195-1750

Received July 14, 2009

Revised Manuscript Received August 29, 2009

π -Conjugated polymer semiconductors are of broad interest for applications in organic electronics and optoelectronics including field-effect transistors and photovoltaic cells.^{1–14} Poly(3-alkylthiophene)s¹ and derivatives^{2,3} are among the most studied organic semiconductors for these applications. Because few conjugated polymer semiconductors combine high carrier mobility with good oxidative stability, various approaches have been explored to improve oxidative stability while retaining high performance in devices.^{2–5} Incorporation of aromatic or aromatic heterocyclic rings into a polythiophene backbone by copolymerization represents a successful strategy, leading to polymer semiconductors with enhanced oxidative stability and higher carrier mobilities compared to the parent poly(3-alkylthiophene)s.^{3–5} Aromatic heterocyclic rings such as thiazolothiazole,^{4a–c} 5,5'-bithiazole,^{4d} thienopyrazine,^{5a} and thieno-thiophenes³ exemplify this approach, which is successful largely by enhancing intermolecular π -stacking interactions and long-range 3-D or 2-D order in the solid state.^{1–5,12}

Benzobisthiazole and benzobisoxazole polymers and small molecules are well-known to exhibit efficient π -stacking and strong intermolecular interactions in the solid state,⁷ leading to high-temperature resistance with glass transition temperatures that can exceed 300–400 °C and relatively high electron affinity.^{8–10} However, polybenzobisthiazoles and polybenzobisoxazoles have mainly been previously explored as electron transport materials in organic light-emitting diodes and as nonlinear optical materials.^{9,10} Earlier limited studies of a benzobisthiazole polymer as an n-channel semiconductor in field-effect transistors observed a low mobility of electrons,^{11a} requiring a high electron affinity polymer^{11b} in a blend to achieve electron injection. Recently, thin film transistors from benzobisthiazole small molecules were reported to exhibit high field-effect mobilities of holes and electrons.¹²

We report herein the synthesis and characterization of a new organic solvent soluble benzobisthiazole–thiophene copolymer based on alternating benzobisthiazole and oligo-3-octylthiophene units in the backbone, poly(benzobisthiazole-*alt*-3-octylthiophene) (PBTOT). The incorporation of benzobisthiazole into a regioregular poly(3-alkylthiophene) is designed to improve oxidative stability by increasing the ionization potential (IP), thermal stability, interchain interactions and thus enhance the charge transport properties of the polymers. The new copolymer semiconductor indeed shows an increased ionization potential and robust thermal and air stability. The highly crystalline PBTOT thin films exhibit a field-effect carrier mobility of up

to 0.01 cm²/(V s) and bulk heterojunction solar cells made from PBTOT have a power conversion efficiency of 2.1% under 100 mW/cm² AM1.5 sunlight in ambient air. The field-effect carrier mobility and photovoltaic properties of PBTOT are substantially enhanced compared to the related regioregular poly(3-octylthiophene) (P3OT).^{13,14}

Synthesis and Characterization. Scheme 1 shows the synthetic route to PBTOT and the required monomers. Monomer **5** was prepared according to a reported literature method.^{4a,15} Alkyl-substituted bis(2-thienyl)benzobisthiazole monomer **3** was prepared by acid-catalyzed condensation of aldehyde **1**^{4c} and 2,5-diamino-1,4-benzenedithiol dihydrochloride (**2**) in 12% yield. Bromination of **3** using NBS provided monomer **4** in 84% yield. Copolymerization of monomers **4** and **5** was carried out by Stille coupling reaction using Pd₂(dba)₃ and P(*o*-Tol)₃ as catalyst and ligand in chlorobenzene^{5a} (Scheme 1). The polymer was purified by Soxhlet extraction with methanol and hexane. Two fractions of PBTOT were isolated based on the molecular weight as shown in Table 1. PBTOT-1 was extracted from chloroform as a shiny green solid, and PBTOT-2 was extracted from 1,2-dichlorobenzene as a shiny green solid. The molecular weight of PBTOT was determined by gel-permeation chromatography (GPC) in chlorobenzene solution relative to polystyrene standards. PBTOT-1 has a weight-average molecular weight (M_w) of 15 400 and a polydispersity index (PDI) of 1.91. It is soluble in organic solvents such as chloroform, chlorobenzene, and dichlorobenzene. A second sample PBTOT-2 has a high weight-average (M_w = 722 000, PDI = 1.97) and is only soluble in hot 1,2-dichlorobenzene and 1,2,4-trichlorobenzene. The rather high molecular weight of PBTOT-2 limits its solubility in more organic solvents. Differential scanning calorimetry (DSC) showed a melting peak (T_m) at 367 °C and recrystallization (T_c) at 356 °C for PBTOT-2 and slightly lower melting transition for PBTOT-1 (T_m of 290 °C and T_c of 265 °C). A glass transition temperature was not observed in the DSC scans of PBTOT. The T_m of PBTOT is dramatically enhanced compared to the 200–205 °C melting transition temperature in P3OT.^{1b}

Photophysics. The normalized optical absorption spectra of thin films of PBTOT are shown in Figure 1. PBTOT-1 has an absorption maximum (λ_{max}) at 540 nm, whereas PBTOT-2 has a well-defined vibronic structure with an absorption maximum at 551 nm and a red-shifted shoulder at 600 nm, an indication of strong interchain interactions in the solid state. When a thin film of PBTOT-1 was annealed at 150 °C, a lower energy shoulder appeared at 580 nm, indicating improved interchain interactions (Figure S3). In the case of PBTOT-1, the absorption maximum in dilute 1,2-dichlorobenzene solution was at 490 nm, which is ~50 nm blue-shifted compared to the thin-film absorption, indicating increased planarization and improved π -stacking in the solid state (Figure S2A). PBTOT-2 showed an absorption maximum of 537 nm in dilute hot 1,2-dichlorobenzene. The optical band gap from the PBTOT absorption edge of the thin films was 1.94–1.97 eV. These values are slightly higher than P3OT (1.9 eV) band gap. This result is unusual for donor–acceptor copolymers, suggesting that there is no significant intramolecular charge transfer.^{5a–c} The photoluminescence (PL) emission spectrum of PBTOT-1 in dilute 1,2-dichlorobenzene solution has a vibronic structure with a maximum at 573 nm, whereas PBTOT-2 in solution has a maximum at 630 nm (Figure S2B). In the solid state, both

*Corresponding author. E-mail: jenekhe@u.washington.edu.

Scheme 1. Chemical Structure and Synthetic Route to PBTOT

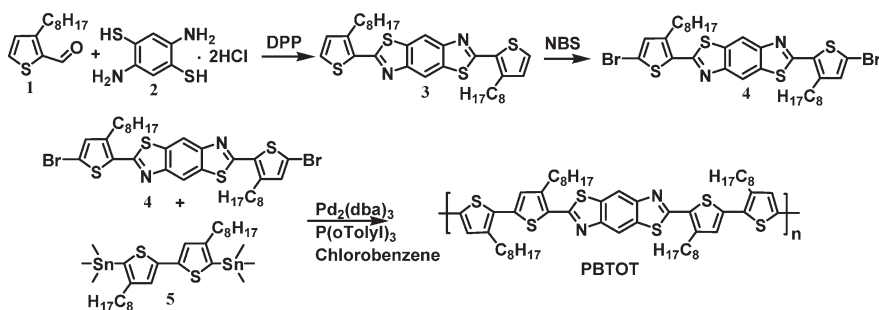


Table 1. Molecular Weight and Thermal, Optical, and Electrochemical Properties of PBTOT

polymer	M_w	PDI	T_m/T_c (°C)	λ_{max} (film, nm)	E_g^{opt} (eV)	IP (eV)	EA (eV)
PBTOT-1	15 400	1.91	290/265	540	1.97	5.2	3.3
PBTOT-2	722 000	1.97	367/356	551	1.94		

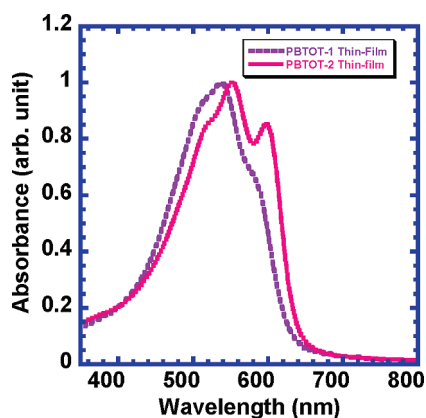


Figure 1. Normalized absorption spectra of thin films of PBTOT.

PBTOT-1 and PBTOT-2 had red emission with a PL maximum at 687–690 nm (Figure S2B).

Electrochemistry. Cyclic voltammetry of PBTOT-1 thin-films showed quasi-reversible oxidation whereas a reduction wave was not observed. The onset oxidation potential was 0.80 V (vs SCE) corresponding to a highest occupied molecular orbital (HOMO) of 5.2 eV. The lowest unoccupied molecular orbital (LUMO) was roughly estimated to be 3.3 eV by using the optical band and the relation $LUMO = HOMO - E_g^{opt}$ (Table 1). The HOMO level of PBTOT is 0.3 eV lower than P3OT (4.9 eV). This is clearly a result of incorporating the electron-deficient benzobisthiazole moiety into P3OT backbone. The HOMO/LUMO energy levels of PBTOT suggest that it should be stable hole transporting material. PBTOT is oxidatively more stable than either P3OT or P3HT. Although the benzobisthiazole unit seems to have only a small effect on the optical band gap, it has clearly shifted the HOMO and LUMO levels by 0.3 eV.

Morphology and Molecular Packing. To investigate the solid-state morphology and molecular organization of PBTOT, we performed X-ray diffraction (XRD) analysis on thin films drop-casted from a 1,2-dichlorobenzene solution onto glass substrates and dried overnight in a vacuum oven (60 °C). The XRD spectrum of PBTOT-2 film is shown in Figure 2A. Diffraction peaks are observed at $2\theta = 5.66^\circ$ (100), 11.1° (200), and 16.4° (300), indicating a high degree of crystallinity in the PBTOT-2 films. The XRD spectrum of PBTOT-1 film also showed similar reflections, with peaks at $2\theta = 5.58^\circ$ (100) and 11.1° (200) (Figure S6). The diffraction

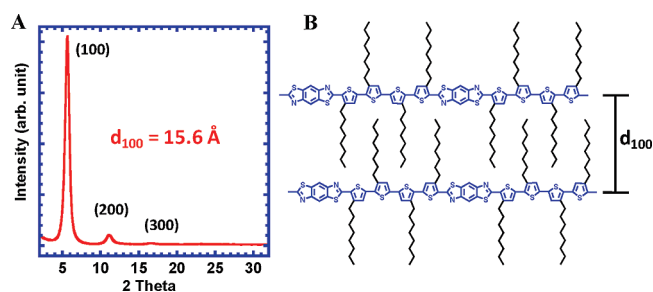


Figure 2. XRD spectrum of PBTOT-2 thin film (A) and proposed packing structure (B).

peak at 5.66° corresponds to an interlayer lamellar d_{100} -spacing of 15.6 Å, which is much smaller than that of P3OT (20.1 Å).^{1b} In addition, the interchain lamellar d_{100} -spacing of PBTOT is even smaller than that of P3HT (16.3 Å).^{1b} It is known that there are two common packing modes of alkyl-chain-substituted polymers: interdigitation and end-to-end packing.^{1–3,4a–d} The observed interlayer distance suggests that the alkyl chains of PBTOT interdigitate as illustrated in Figure 2B. The film morphology of PBTOT was also examined by atomic force microscopy (AFM) on thin films spin-coated onto glass substrates without annealing. Nodule-like structures were observed in the surface morphology revealed by AFM images (Figure S5).

Field-Effect Transistors. The charge transport properties of PBTOT were investigated by fabricating OFETs with conventional bottom-contact and bottom-gate geometry on top of silicon (gate) and silicon dioxide (dielectric) substrates and patterned gold source/drain electrodes. The typical output and transfer characteristics of PBTOT OFETs are shown in Figure 3, and the results are summarized in Table 2. An average hole mobility (μ_h) of $0.009 \text{ cm}^2/(\text{V s})$ and a maximum hole mobility of $0.01 \text{ cm}^2/(\text{V s})$ were observed for PBTOT-2. The I_{on}/I_{off} ratios were higher than 10^6 , and the threshold voltage (V_t) was -5.2 V (Table 2). The highly crystalline nature of PBTOT, as revealed in the absorption spectra and XRD patterns, facilitates good charge transport in the thin films. The lower molecular weight fraction (PBTOT-1) had a hole mobility of $0.002 \text{ cm}^2/(\text{V s})$, I_{on}/I_{off} ratio of 10^5 , and a threshold voltage of -19 V . Thus, the hole mobility is increased by a factor of 5 when the molecular weight is increased from 15.4 to 722 kDa. The enhanced charge carrier mobility and overall better OFET performance in the higher molecular weight polymer is likely due

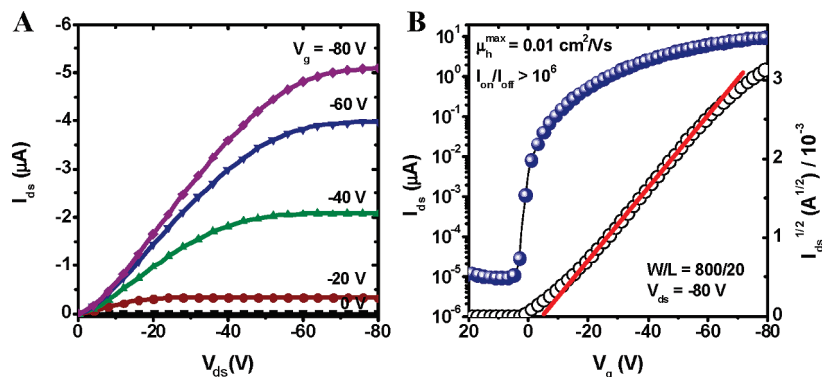


Figure 3. Output (A) and transfer (B) characteristics of a PBTOT-2 OFET.

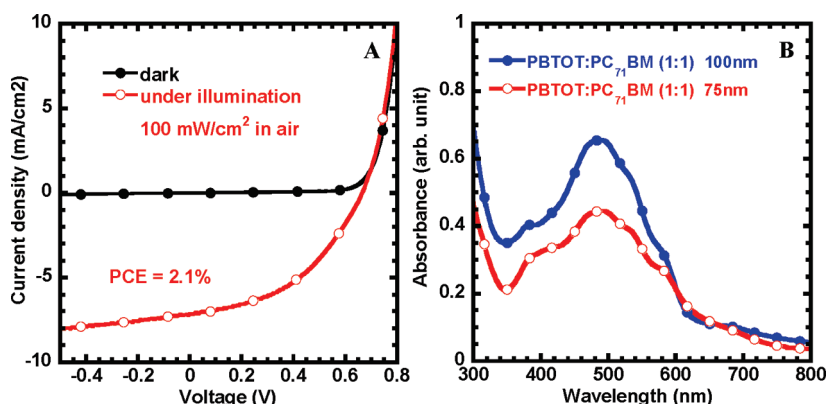


Figure 4. (A) Current density–voltage curves of a PBTOT-1:PC₇₁BM (1:1) device under 100 mW/cm² AM1.5 solar irradiation and in the dark. (B) Optical absorption spectra of PBTOT-1:PC₇₁BM (1:1) blend films on glass/ITO/PEDOT substrates.

Table 2. Electrical Parameters of PBTOT-Based OFETs and Solar Cells

polymer	μ_h (cm ² /(V s))	I_{on}/I_{off}	V_t (V)	J_{sc} (mA/cm ²)	V_{oc}	FF	PCE (%)
PBTOT-1	0.002	$>10^5$	-19	7.08	0.66	0.45	2.1
PBTOT-2	0.01	$>10^6$	-5.2				

in part to reduction in defects arising from chain ends and enhancement in interchain interactions. Remarkably, the observed 0.01 cm²/(V s) mobility of holes in PBTOT-2 is much higher than the (2.0–13.0) × 10⁻⁴ cm²/(V s) reported for regioregular P3OT thin films.¹³ PBTOT-2 devices under ambient conditions showed remarkable air stability. The average hole mobility of PBTOT-2 OFETs in air was 0.007 cm²/(V s), which remained unchanged for 54 days. The on/off ratio and threshold voltage similarly remained very good at 10⁶ and -12 V, respectively.

Solar Cells. We fabricated and characterized bulk heterojunction (BHJ) solar cells based on blends of PBTOT-1 and PC₇₁BM in photodiodes with the structure ITO/PEDOT:PSS/blend/LiF/Al. The higher molecular weight sample, PBTOT-2, was not sufficiently soluble in 1,2-dichlorobenzene to achieve reasonable film thickness (60–100 nm) for the fabrication of BHJ devices. The current density–voltage characteristics of the PBTOT-1:PC₇₁BM (1:1) blend solar cell under dark and under 100 mW/cm² AM1.5 solar illumination are shown in Figure 4A. The associated photovoltaic parameters, including the short-circuit current density (J_{sc}), the open-circuit voltage (V_{oc}), the fill factor (FF), and power conversion efficiency (PCE), are summarized in Table 2. The combination of fairly large photocurrent (7.08 mA/cm²) with a good open-circuit voltage (0.66 V) translates to a 2.1% PCE. Considering the relatively narrow

absorption bands of the PBTOT-1:PC₇₁BM blends (Figure 4B) and unoptimized nature of the BHJ solar cells with respect to blend composition, active layer film thickness, and molecular weight, we conclude that benzobisthiazole–thiophene copolymer semiconductors are promising for photovoltaic cells.

Conclusions. In summary, we have synthesized and characterized a new donor–acceptor copolymer semiconductor based on benzobisthiazole as the acceptor unit and 3-octyl-quarterthiophene as the donor unit. X-ray diffraction of PBTOT films showed a crystalline lamellar structure with an interlayer d_{100} -spacing of 15.6 Å, which is substantially shorter than the interlayer d_{100} -spacing of 20.1 Å in regioregular poly(3-octylthiophene) (P3OT). Among consequences of the enhanced interchain interactions in PBTOT include the much higher melt transition temperature and improved field-effect charge transport compared to P3OT. Preliminary studies of PBTOT-based OFETs showed carrier mobility as high as 0.01 cm²/(V s) and on/off current ratios of 10⁶. Initial bulk heterojunction solar cells based on the blends of the low molecular weight PBTOT-1 with PC₇₁BM had a power conversion efficiency of 2.1% under 100 mW/cm² AM1.5 solar illumination in air. Ongoing work is exploring the synthesis of various benzobisthiazole-based donor–acceptor copolymers for organic electronics.

Acknowledgment. Our work was supported by the NSF (DMR 0805259 and DMR 0120967) and the DOE Basic Energy Sciences (DE-FG02-07ER46467). This work was supported in part by Solvay S. A.

Supporting Information Available: Experimental, ¹H NMR spectra, solution UV–vis and PL spectra, DSC scans, cyclic

voltammogram scans, AFM images, and X-ray diffraction spectrum. This material is available free of charge via the Internet at <http://pubs.acs.org>.

References and Notes

- (1) (a) McCullough, R. D.; Tristram-Nagle, S.; Williams, S. P.; Lowe, R. D.; Jayaraman, M. *J. Am. Chem. Soc.* **1993**, *115*, 4910. (b) Chen, T.-A.; Wu, X.; Rieke, R. D. *J. Am. Chem. Soc.* **1995**, *117*, 233. (c) Bao, Z.; Dobablapur, A.; Lovinger, A. J. *Appl. Phys. Lett.* **1996**, *69*, 4108. (d) Sirringhaus, H.; Tessler, N.; Friend, R. H. *Science* **1998**, *280*, 1741. (e) Babel, A.; Jenekhe, S. A. *J. Phys. Chem. B* **2003**, *107*, 1749.
- (2) Ong, B. S.; Wu, Y.; Gardner, S. *J. Am. Chem. Soc.* **2004**, *126*, 3378.
- (3) (a) McCulloch, I.; Heeney, M.; Bailey, C.; Genevicius, K.; Macdonald, I.; Shkunov, M.; Sparrowe, D.; Tierney, S.; Wagner, R.; Zhang, W.; Chabinyc, M. L.; Kline, R. J.; McGehee, M. D.; Toney, M. F. *Nat. Mater.* **2006**, *5*, 328. (b) Li, Y.; Wu, Y.; Liu, P.; Birau, M.; Pan, H.; Ong, B. S. *Adv. Mater.* **2006**, *18*, 3029. (c) Pan, H.; Wu, Y.; Li, Y.; Ong, B. S.; Zhu, S.; Gu, X. *Adv. Funct. Mater.* **2007**, *17*, 3574. (d) Heeney, M.; Bailey, C.; Genevicius, K.; Shkunov, M.; Sparrowe, D.; Tierney, S.; McCulloch, I. *J. Am. Chem. Soc.* **2005**, *127*, 1078.
- (4) (a) Osaka, I.; Zhang, R.; Sauve, G.; Smilgies, D.-M.; Kowalewski, T.; McCullough, R. D. *J. Am. Chem. Soc.* **2009**, *131*, 2521. (b) Osaka, I.; Sauve, G.; Zhang, R.; Kowalewski, T.; McCullough, R. D. *Adv. Mater.* **2007**, *19*, 4160. (c) Narazo, Wudl, F. *Macromolecules* **2008**, *41*, 3169. (d) Kim, D. H.; Lee, B.-L.; Moon, H.; Kang, H. M.; Jeong, E. J.; Park, J.-L.; Han, K.-M.; Lee, S.; Yoo, W. B.; Koo, B. W.; Kim, Y.; Lee, W. H.; Cho, K.; Becerril, H. A.; Bao, Z. *J. Am. Chem. Soc.* **2009**, *131*, 6124. (e) Yang, C.; Cho, S.; Chiechi, R. C.; Walker, W.; Coates, N. E.; Daniel, M.; Heeger, A. J.; Wudl, F. *J. Am. Chem. Soc.* **2008**, *130*, 16524. (f) He, Y.; Wang, X.; Zhang, J.; Li, Y. *Macromol. Rapid Commun.* **2009**, *30*, 45.
- (5) (a) Zhu, Y.; Champion, R. D.; Jenekhe, S. A. *Macromolecules* **2006**, *39*, 8712. (b) Wu, P.-T.; Kim, F. S.; Champion, R. D.; Jenekhe, S. A. *Macromolecules* **2008**, *41*, 7021. (c) Guo, X.; Kim, F. S.; Jenekhe, S. A.; Watson, M. D. *J. Am. Chem. Soc.* **2009**, *131*, 7206. (d) Zhang, M.; Tsao, H. N.; Pisula, W.; Yang, C.; Mishra, A. K.; Müllen, K. *J. Am. Chem. Soc.* **2007**, *129*, 3472. (e) Tsao, H. N.; Cho, D.; Andreasen, J. W.; Rouhanipour, A.; Breiby, D. W.; Pisula, W.; Müllen, K. *Adv. Mater.* **2009**, *21*, 209.
- (6) (a) Xin, H.; Kim, F. S.; Jenekhe, S. A. *J. Am. Chem. Soc.* **2008**, *130*, 5424. (b) Xin, H.; Kim, F. S.; Ren, G.; Jenekhe, S. A. *Chem. Mater.* **2008**, *20*, 6199.
- (7) (a) Jenekhe, S. A.; Osaheni, J. A. *Science* **1994**, *265*, 765. (b) Osaheni, J. A.; Jenekhe, S. A. *J. Am. Chem. Soc.* **1995**, *117*, 7389. (c) So, Y.-H.; Zaleski, J. M.; Murlick, C.; Ellaboudy, A. *Macromolecules* **1996**, *29*, 2783. (d) Mike, J. F.; Makowski, A. J.; Jeffries-EL, M. *Org. Lett.* **2008**, *10*, 4915.
- (8) (a) Wolfe, J. F.; Loo, B. H.; Arnold, F. E. *Macromolecules* **1981**, *14*, 915. (b) Choe, E. W.; Kim, S. N. *Macromolecules* **1981**, *14*, 920. (c) Roberts, M. F.; Jenekhe, S. A. *Chem. Mater.* **1993**, *5*, 1744. (d) Osaheni, J. A.; Jenekhe, S. A. *Chem. Mater.* **1995**, *7*, 672.
- (9) (a) Osaheni, J. A.; Jenekhe, S. A. *Macromolecules* **1993**, *26*, 4726. (b) Alam, M. M.; Jenekhe, S. A. *Chem. Mater.* **2002**, *14*, 4775.
- (10) (a) Jenekhe, S. A.; Osaheni, J. A.; Meth, J. S.; Vanherzeele, H. *Chem. Mater.* **1992**, *4*, 683. (b) Osaheni, J. A.; Jenekhe, S. A. *Chem. Mater.* **1992**, *4*, 1282. (c) Dotrong, M.; Mehta, R.; Balchin, G. A.; Tomlinson, R. C.; Sinsky, M.; Lee, C. Y. C.; Evers, R. C. *J. Polym. Sci., Part A* **1993**, *31*, 723.
- (11) (a) Babel, A.; Jenekhe, S. A. *J. Phys. Chem. B* **2002**, *106*, 6129. (b) Babel, A.; Jenekhe, S. A. *J. Am. Chem. Soc.* **2003**, *125*, 13656.
- (12) (a) Pang, H.; Vilela, F.; Skabara, P. J.; McDouall, J. J. W.; Crouch, D. J.; Anthopoulos, T. D.; Bradley, D. D. C.; de Leeuw, D.; Horton, P. N.; Hursthouse, M. B. *Adv. Mater.* **2007**, *19*, 4438. (b) Mamada, M.; Nishida, J.-I.; Tokito, S.; Yamashita, Y. *Chem. Lett.* **2008**, *37*, 766.
- (13) (a) Babel, A.; Jenekhe, S. A. *Synth. Met.* **2005**, *148*, 169. (b) Zen, A.; Saphiannikova, M.; Neher, D.; Asawapirom, U.; Scherf, U. *Chem. Mater.* **2005**, *17*, 781.
- (14) (a) Al-Ibrahim, M.; Roth, H.-K.; Schroedner, M.; Konkin, A.; Zhokhavets, U.; Gobsch, G.; Scharff, P.; Sensfuss, S. *Org. Electron.* **2005**, *6*, 65. (b) Nguyen, L. H.; Hoppe, H.; Erb, T.; Günes, S.; Gobsch, G.; Sariciftci, N. S. *Adv. Funct. Mater.* **2006**, *17*, 1071. (c) Gebeyehu, D.; Brabec, C. J.; Padinger, F.; Fromherz, T.; Hummelen, J. C.; Badt, D.; Schindler, H.; Sariciftci, N. S. *Synth. Met.* **2001**, *118*, 1.
- (15) Zagorska, M.; Krische, B. *Polymer* **1980**, *31*, 1379.